

Spin quantum tunneling in single molecular magnets: fingerprints in transport spectroscopy of current and noise

C. Romeike, M. R. Wegewijs, and H. Schoeller
Institut für Theoretische Physik A, RWTH Aachen,
52056 Aachen, Germany
 (Dated: November 18, 2018)

We demonstrate that transport spectroscopy of *single* molecular magnets shows signatures of quantum tunneling at low temperatures. We find current and noise oscillations as function of bias voltage due to a weak violation of spin selection rules by quantum tunneling processes. The interplay with Boltzmann suppression factors leads to fake resonances with temperature-dependent position which do not correspond to any charge excitation energy. Furthermore, we find that quantum tunneling can completely suppress transport if the transverse anisotropy has a high symmetry.

PACS numbers: 85.65.+h, 73.23.Hk, 73.63.Kv

Introduction. Single molecular magnets (SMM) have become famous in the last decade for showing the quantum tunneling of a single magnetic moment (QTM) on a macroscopic scale [1, 2, 3, 4, 5, 6]. These molecules are characterized by a large spin $S > \frac{1}{2}$, a large magnetic anisotropy barrier (MAB) and anisotropy terms which allow this spin to tunnel through the barrier. The anisotropy is due to spin-orbit effects on the metal-ions whose spins couple to form the large magnetic moment. Magnetic hysteresis, associated with QTM, was observed at temperatures below the MAB [1, 2] for ensembles of molecules in a single crystal. Recently, Cornia et al. [7] were able to immobilize *single* SMMs on a gold surface through modification of their ligands while preserving the magnetic properties of the core. Using this technique Heersche et al. [8] were able to establish a 3-terminal electrical contact and measure the transport through the well-known SMM Mn12, see also [9].

In this Letter we show that transport spectroscopy of single molecular magnets can reveal specific features being fingerprints of spin quantum tunneling. Even when the anisotropy terms which cause QTM have a small effect on the energy spectrum they lead to significant changes in the *non-equilibrium occupations of the magnetic states* since they allow for a violation of spin-selection rules for electron-tunneling. As a consequence, QTM leads to an oscillatory behavior of the current and shot-noise with increasing bias voltage. Specifically, the interplay of several small rates (quantum tunneling induced rates and rates suppressed by Boltzmann factors) leads to negative differential conductance and, most strikingly, to the occurrence of so-called fake resonances which do *not* correspond to any charge excitation energy. The fake resonance's position depends on temperature, and allows a clear experimental identification of quantum tunneling processes. Furthermore, we show that high symmetry (due to the molecular structure) QTM can give rise to a complete current suppression.

Theory. We analyze a minimal model that combines the well-known effective spin Hamiltonian description of SMMs [10, 11, 12, 13, 14] with the standard tunneling Hamiltonian for the coupling to metallic electrodes. Due

to the high charging energy it is sufficient to consider only two charge states ($N = 0, 1$) with a magnetic excitation spectrum $H^{(N)} = H_{\text{MAB}}^{(N)} + H_{\text{QTM}}^{(N)}$, where

$$H_{\text{MAB}}^{(N)} = -D^{(N)}(\hat{S}_z)^2 \quad (1)$$

$$H_{\text{QTM}}^{(N)} = -\frac{1}{2} \sum_{n=1,2} B_{2n} \left[(\hat{S}_+^2)^n + (\hat{S}_-^2)^n \right]. \quad (2)$$

(We employ units $\hbar = e = k_B = 1$ and energy units of meV). For each charge state N the spin has a definite value $S^{(N)}$ and spin projection $|M| \leq S^{(N)}$ which is maximal in the ground state. The anisotropy terms arise due to spin-orbit interaction on the molecule and break rotational invariance in spin-space. The lowest order easy-axis anisotropy in Eq. (1) defines the preferred axis in space along which we quantize the spin (z -axis). The eigenstates $|N, S, M\rangle$ of Eq. (1) have an inverted parabolic energy dependence depicted in Fig. 1(a). Higher order corrections to the magnetic anisotropy barrier are not essential here. It is known experimentally [15, 16, 17, 18, 19, 20, 21] and theoretically [14] that the anisotropy constants $D^{(N)}$ depend on the charge state. The transverse anisotropy, Eq. (2), accounts for deviations from purely axial symmetry. We consider either a second or fourth ($n = 1$ or 2) order term which allows for tunneling of the spin between states with M values differing by $2n$. (It is convenient here to deviate from the conventional notation $E = B_2$ and $C = B_4$). Since a charge-dependent QTM induces only small corrections in the spectrum of the molecule B_{2n} is taken as charge-independent. Transport through SMMs provides information on the magnetic structure in more than one charge state of the molecule. Therefore we investigate the basic possible combinations of the magnetic parameter values for charged SMMs which are scarcely known. Also, in a single-molecule junction they may change due to mechanical and electrostatic effects. Below we select our values from the typical range $D^{(N)} \sim 0.01 - 0.1 \text{ meV}$, $B_2 \sim 10^{-3} - 10^{-7} \text{ meV}$ and $B_4 \sim 10^{-4} - 10^{-7} \text{ meV}$ for which magnetic excitations can be resolved in the transport at electron temperatures below 1 K. Since QTM

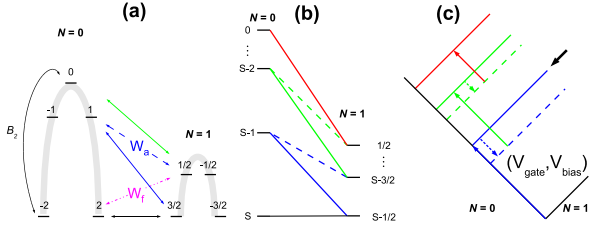


FIG. 1: (a) Magnetic excitation spectra for two charge states with spins $S^{(0)} = 2 > S^{(1)} = 3/2$ and $D^{(0)} > D^{(1)}$. Since typically $B_{2n} \ll D^{(N)}$ we label the eigenstates by the approximately good quantum number M . The dot-dashed line is a spin-forbidden transition, all others are spin-allowed. (b) Energy levels and spin-allowed transitions for $S^{(0)} = S > S^{(1)} = S - \frac{1}{2}$. (c) Electron-addition excitations in $(V_{\text{gate}}, V_{\text{bias}})$ stability diagram. Arrows indicate how to construct the diagram going along the zig-zag path in (b). Thick/thin lines indicate visible/hidden transitions. A transition is hidden when the initial state is not yet occupied (by other processes) at the transition energy.

weakly affects the energy spectrum we will label eigenstates of $H^{(N)}$ by the approximately good quantum number M , i.e. state $|N, S, M\rangle$ has the largest contribution. The electrodes $r = L, R$ are described as electron reservoirs with electrochemical potential $\mu \pm V_{\text{bias}}/2$ and a constant density of states ρ : $H_{\text{res}} = \sum_{rk\sigma} (\epsilon_{k\sigma r} - \mu_r) c_{rk\sigma}^\dagger c_{rk\sigma}$. The tunneling term $H_{\text{mol-res}} = \sum_{rkj\sigma} t_j d_{j\sigma}^\dagger c_{rk\sigma} + h.c.$ describes charge transfer between electrode and molecule (symmetric tunneling barriers). Here $d_{j\sigma}^\dagger$ adds an electron with spin σ to a single-particle orbital on the molecule. The coupling to a gate electrode is included in a shift of the molecular energies, such that the charge degeneracy point is at zero bias (V_{bias}) and gate voltage (V_{gate}). For weak tunneling, we use a standard master equation approach to calculate the non-equilibrium occupations of the molecular states, the current and the shot noise [22]. The rates in this master equation are calculated in golden rule approximation. For the transition $s_2 \rightarrow s_1$ (s_i being two eigenstates of $H^{(N_i)}$ with energy E_i), we obtain the total rate $W_{s_1, s_2} = \sum_r W_{s_1, s_2}^{r,+} + W_{s_1, s_2}^{r,-}$ with the tunneling-in rate $W_{s_1, s_2}^{r,+} = 2\pi\rho \sum_\sigma f_r(E_{s_1} - E_{s_2}) |T_{s_1 s_2}^\sigma|^2$ and the tunneling-out rate $W_{s_1, s_2}^{r,-} = 2\pi\rho \sum_\sigma (1 - f_r(E_{s_1} - E_{s_2})) |T_{s_2 s_1}^\sigma|^2$. Here, $f_r(E) = (e^{(E - \mu_r)/T} + 1)^{-1}$ is the Fermi function of reservoir r , T denotes the temperature, and $T_{s_1 s_2}^\sigma = \sum_j t_j \langle s_1 | d_{j\sigma}^\dagger | s_2 \rangle$. These tunnel matrix elements incorporate the spin selection rules and their violation for finite QTM. Without QTM, the eigenstates are given by $|s_i\rangle = |N_i, S_i, M_i\rangle$, and the tunnel matrix elements fulfill obviously the spin selection rule $|S_1 - S_2| = 1/2$ and $|M_1 - M_2| = 1/2$, in addition to $|N_1 - N_2| = 1$. For weak QTM, we decompose the states s_i into a linear combination of $|N_i, S_i, M_i\rangle$ states, the one with largest contribution being $M'_i = M_i$. Inserting this expansion into $T_{s_1 s_2}^\sigma$ leads to a summation of matrix ele-

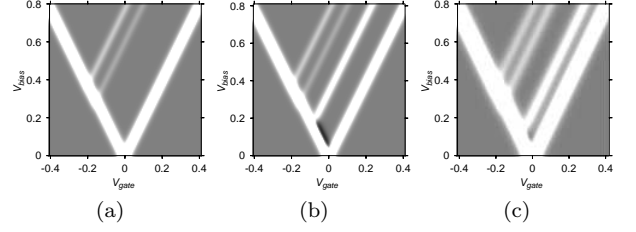


FIG. 2: dI/dV_{bias} in gray-scale (gray= zero, white/black = positive/negative) as function of V_{gate} and V_{bias} . Parameters: $S^{(0)} = 2, S^{(1)} = 3/2, D^{(0)} = 0.1, D^{(1)} = 0.01$ and $T = 0.01$. (a) No QTM: $B_2 = 0$. (b) QTM $B_2 = 2 \times 10^{-5}$ (c) Same as (b) except for higher $T = 0.015$.

ments with terms $\langle N_1, S_1, M'_1 | \sum_j t_j d_{j\sigma}^\dagger | N_2, S_2, M'_2 \rangle$. Using the Wigner-Eckart theorem, each of these matrix element can be factorized into an M -dependent Clebsch-Gordan (CG) coefficient and a common constant c_j . Each individual CG-coefficient fulfils $|S_1 - S_2| = 1/2$ and $|M'_1 - M'_2| = 1/2$. Obviously the overall spin selection rule $|M_1 - M_2| = 1/2$ can be weakly violated, i.e. the corresponding rate is smaller by roughly a factor $(B_{2n}/D^{(N)})^2$ compared to the rates fulfilling the overall spin selection rule. The constants c_j are incorporated into a factor $\Gamma = 2\pi\rho |\sum_j t_j c_j|^2$ common to all rates and drop out of the problem, except for setting the absolute current and noise scale. We note that, in contrast to customary spin-blockade physics [23], a complete elimination of the spin projection M from the transport problem is not possible due to the MAB and QTM. The master equation approach correctly accounts for both the non-equilibrium induced by the electron tunneling at finite bias voltage and the thermal excitation of molecular spin-states. The life-time of the latter is also limited by other relaxation processes (spin-phonon interaction, nuclear spins, etc.) which are typically [24] slower than electron tunneling processes (time $\lesssim 1$ ns) and are therefore neglected. Furthermore, the spin-phonon interaction may be hindered since the phonon spectrum for a single molecule is expected to be less dense than in a bulk system.

Fake resonances and oscillations. To illustrate the effect of the QTM on the transport we first explain the conductance map for small spins ($S^{(0)} = 2, S^{(1)} = 3/2$) and contrast the cases $B_2 = 0$ and $B_2 \neq 0$. For $B_2 = 0$ the differential conductance map is plotted in Fig. 2(a) and we discuss the resonance lines running upward. Starting at the charge degeneracy point ($V_{\text{gate}} = V_{\text{bias}} = 0$) and increasing the bias voltage the current initially sets on due to the ground state transitions $M = \pm 2 \leftrightarrow M' = \pm 3/2$, see Fig. 1(a). Increasing the bias voltage further brings the transition $M = \pm 2 \leftrightarrow M' = \pm 1/2$ into the transport energy window, without any effect on the current: the rate for the process vanishes due to spin selection rules, $W_f = 0$ [dot-dashed in Fig. 1(a)]. A reservoir spin-1/2 electron can not couple two molecular states with $|\Delta M| > 1/2$.

Therefore this resonance is hidden [25, 26]. The current only increases when the transition $M = \pm 1 \leftrightarrow M' = \pm 3/2$ becomes energetically allowed. At this resonance all states except $N = 0, M = 0$ become occupied equally. At the third resonance the latter state also becomes accessible via $M = 0 \leftrightarrow M' = \pm 1/2$. In the presence of QTM, $B_2 \neq 0$, two additional resonances appear, see Fig. 2(b), one with positive and one with negative dI/dV_{bias} . The appearance of negative dI/dV_{bias} is related to a slow, spin-forbidden transition as follows. For $B_2 \ll D$ the spin-projection M is only approximately a good quantum number, i.e. each eigenstate is a linear combination of states $\{|N, S, M + 2k\rangle\}_{k=0, \pm 1, \pm 2, \dots}$, with one coefficient ($k = 0$) close to 1. In the $N = 1$ excited state in addition to the state $M' = \pm 1/2$, there is thus a small admixture $\propto B_2/D^{(1)}$ of state $M = \mp 3/2$. The forbidden transition to the $N = 0$ ground states composed mostly of $M = \pm 2$ [Fig. 1(a)] is now weakly allowed. When it becomes energetically allowed the transition occurs with rate $W_f \sim (B_2/D^{(1)})^2\Gamma$ and the current is suppressed. This is simply because the occupation of the $N = 1$ excited states reduces the occupations of the states which contribute most to the transport current through (fast) spin-allowed transitions. In contrast, the positive dI/dV_{bias} line which appears is *not* related to any additional energy of the molecule. The current increase occurs when the state causing the negative differential conductance (NDC) above is depleted at higher bias via a spin-allowed transition $M = \pm 1 \leftarrow M' = \pm \frac{1}{2}$ (dashed in Fig. 1). The rate for this process is $W_a \sim \Gamma f(\Delta E - V_{\text{bias}}/2)$ where ΔE denotes the corresponding transition energy. This depletion sets in when in- and out-going rates become equal i.e. $W_a \sim W_f$. Due to the small factor in W_f this occurs already for $V_{\text{bias}}/2 < \Delta E$ where $W_a \approx \Gamma \exp(-(\Delta E - V_{\text{bias}}/2)/T)$. Equating the rates we obtain the resonance condition $V_{\text{bias}}/2 - \Delta E \propto T \ln(D^{(1)}/B_2)$ which is substantially shifted from the position expected naively ($V_{\text{bias}}/2 = \Delta E$). The shift is linear in temperature and logarithmical in the QTM amplitude [27, 28]. The shift with temperature can be larger than the thermal smearing as illustrated in Fig. 2(c). Thus due to the asymmetry between electron tunneling rate constants intrinsic to an SMM, transport resonances appear even when the molecular level is far away from the electrochemical potential. The strong Coulomb charging effect and energy quantization on the molecule are essential to this effect since they restrict the transport to sequential tunneling through two charge states.

For SMMs with large spin, $S^{(0)} = S^{(1)} + \frac{1}{2} > 2$, the above mechanism leads to *oscillations* in the transport quantities, shown in Fig. 3(a)-(c). At low bias the states of the “flatter” $N = 1$ parabola become occupied via spin-forbidden transitions, see Fig. 3 (a) and the current decreases. The depletion of these states by spin-allowed transitions increases the current again, Fig. 3 (b). Due to the peculiar inverted parabolic energy dependence of the magnetic excitations, this sequence is repeated whenever a new $N = 0$ excitation state can be occupied, see

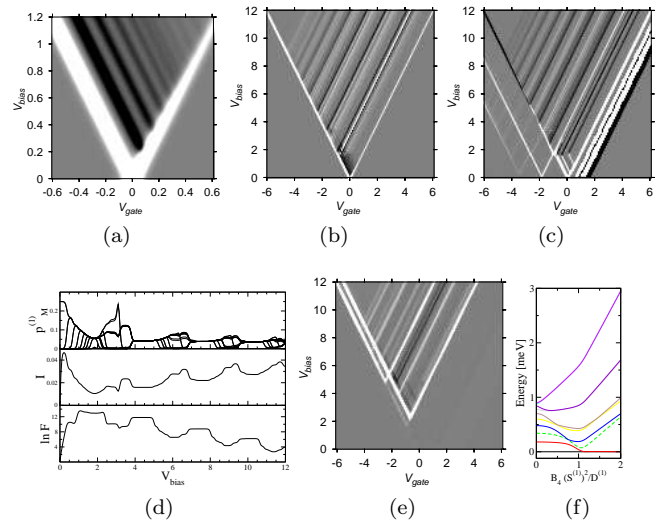


FIG. 3: Transport oscillations induced by QTM. Parameters: $S^{(0)} = 10, S^{(1)} = 9\frac{1}{2}, D^{(0)} = 0.1, D^{(1)} = 0.01, B_2 = 2 \times 10^{-3}$ and $T = 0.015$. (a) dI/dV_{bias} for small bias: the $N = 1$ “flat” parabola is mapped out by NDC excitations. (b) dI/dV_{bias} for large bias: the $N = 0$ excitations give rise to positive and negative differential conductance. (c) $d \ln F/dV_{\text{bias}}$: fake resonance lines correspond to noise suppression (black) lines and terminate at the Coulomb diamond edge. (d) Occupations of the $N = 1$ states $p_M^{(1)}$ together with $\ln F$ and I as function of V_{bias} for $V_{\text{gate}} = 0$. (e) Current suppression due to high-symmetry QTM: $B_4 = 2 \times 10^{-4}, B_2 = 0$. (f) Spin excitation spectrum for the charged state $N = 1$: the value $B_4 S^2/D^{(1)}$ used in (e) lies beyond the level crossing at approximately 1. Only the 2nd excited state has a non-negligible admixture of the maximal $M' = \pm S^{(1)}$ state which is required for transport.

Fig. 1(b)-(c). With increasing bias the $N = 0$ excitations are successively occupied whereas the occupations of the $N = 1$ excitations, and therefore also the current *oscillate*, see Fig. 3(d). Interestingly, all NDC resonances in Fig. 3(a) and (b) correspond to addition energies of the SMM (as in our previous example). Most other resonances with positive differential conductance are fake since they shift with T and B_2 . The *shot-noise* also shows oscillations as function of V_{bias} : in Fig. 3 (c) the Fano-factor $F = S/(2I)$ is plotted. The periodic reductions of F occur due to concerted *reductions of the noise* S and simultaneous *enhancements of the current* I . Their positions shift with T and B_2 and are fake. The noise is super-poissonian, $F \gg 1$, due to the presence of slow and fast tunnel processes that give rise to large current fluctuations [29]. Fig. 3 (d) clearly shows that equal occupation of all $N = 1$ excitations associated with small spin-forbidden tunnel constants reduces the current and simultaneously leads to stronger fluctuations. Depopulation of these states by a spin-allowed transition enhances the current and reduces the noise. Importantly, in Fig. 3(c) the (white) lines of enhanced noise *persist* in the Coulomb blockade regime, in contrast to the fake

(black) lines of noise reduction. The reason for this effect is that the noise in the Coulomb blockade regime will only increase when more excitations lie in the transport window as shown in [29]. Hence measuring shot-noise allows for an identification of fake resonance lines without changing the temperature (which may lead to unwanted changes in the molecular junction). We note that the above is valid also for a weaker magnetic distortion than $D^{(1)}/D^{(0)} < 1/2$ (which is the requirement for the maximum number of oscillations to occur).

High-symmetry anisotropy. When the dominant transverse anisotropy has a high symmetry, i.e. $B_4 \gg B_2/S^2$, and the ratio $B_4/D^{(N)}$ differs for $N = 0$ and $N = 1$ complete current blockade may occur. This is shown in Fig. 3(e) for $S^{(0)} = 10$ and $S^{(1)} = 9\frac{1}{2}$. For $B_4/D^{(1)} \sim 1/S^2$ a level crossing occurs between ground and excited state in the charge sector $N = 1$ [Fig. 3(f)]: the ground states change from a linear combination of $\{|\mp S^{(1)} \pm 4k\rangle_z\}_{k=0,1,\dots}$ to a superposition of $\{|\mp (S^{(1)} - 1) \pm 4k\rangle_z\}_{k=0,1,\dots}$. The latter states have very small tunneling overlap with the $N = 0$ ground state which is a superposition of $\{|\mp S^{(0)} \pm 4k\rangle_z\}_{k=0,1,\dots}$ for sufficiently small $B_4/D^{(0)} \ll 1/S^2$. Thus the transport suppression at low bias signals a high-symmetry QTM perturbation. It can also occur for constant $D^{(0)} \approx D^{(1)} \approx D$ when B_4 changes from smaller than D/S^2 in one charge state to larger than this value. However, if the symmetry of the QTM is also changed by the charging, i.e. the low symmetry QTM becomes important ($B_2 \sim B_4S^2$) in one

charge state, the current blockade can be lifted, since the overlap of ground states is restored. This symmetry lowering may be expected when extra or deficit electrons on the SMM are strongly localized on a particular metal ion contributing to the total spin.

Conclusion. Transport spectroscopy of magnetic molecules is a challenging task since typically many resonances are hidden by spin-selection rules or do not correspond to addition energies of the molecule and shift with temperature. Measuring shot-noise allows for an identification of misleading excitations *without changing the temperature*. If the total spin values are known, a reconstruction of the spectrum from the NDC excitations is possible. Then the fake resonances allow the determination of the quantum tunneling parameter to logarithmic accuracy even though it cannot be resolved directly from the thermally broadened excitations. Finally, we showed that the transport is even sensitive to the symmetry of the magnetic anisotropy of the SMMs. The link we established between transport effects and spin-Hamiltonian parameters may be extended down to the microscopic details of magnetic molecules with further input from ab-initio calculations and energy spectroscopy on charged states of SMMs.

We acknowledge discussions with H. Heersche, J. Kortus, H. van der Zant, and R. Sessoli, and financial support through the Virtual Institute ‘‘Functional Molecular Systems for Information Technology’’ and the EU RTN Spintronics program HPRN-CT-2002-00302.

-
- [1] R. Sessoli, D. Gatteschi, A. Caneschi, and M. A. Novak, *Nature* **365**, 141 (1993).
- [2] J. R. Friedman, M. Sarachick, J. Tejada, and R. Ziolo, *Phys. Rev. Lett.* **76**, 3830 (1996).
- [3] J. M. Hernández, X. X. Zhang, F. Luis, J. Bartolomé, J. Tejada, and R. Ziolo, *Europhys. Lett.* **35** (4), 301 (1996).
- [4] L. Thomas, F. Lioni, R. Ballou, D. Gatteschi, R. Sessoli, and B. Barbara, *Nature* **383**, 145 (1996).
- [5] M. N. Leuenberger and D. Loss, *Phys. Rev. B* **61**, 1286 (2000).
- [6] T. Pohjola and H. Schoeller, *Phys. Rev. B* **62**, 15026 (2000).
- [7] A. Cornia, A. C. Fabretti, M. Pacchioni, L. Zoppi, D. Bonacchi, A. Caneschi, D. Gatteschi, R. Biagi, U. D. Pennino, V. D. Renzi, et al., *Angew. Chem. Int. Ed.* **42**, 1645 (2003).
- [8] H. B. Heersche, Z. de Groot, J. A. Folk, H. S. J. van der Zant, C. Romeike, M. R. Wegewijs, L. Zoppi, D. Barreca, E. Tondello, and A. Cornia, *cond-mat/0510732*.
- [9] M.-H. Jo, J. E. Grose, M. M. Deshmukh, J. J. S. M. Rumberger, D. N. Hendrickson, J. R. Long, H. Park, and D. C. Ralph, *cond-mat/0603276*.
- [10] M. R. Pederson and S. N. Khanna, *Phys. Rev. B* **60**, 9566 (1999).
- [11] M. R. Pederson, D. Porezag, J. Kortus, and S. N. Khanna, *J. Appl. Phys.* **87**, 5487 (2000).
- [12] J. Kortus, T. Baruah, N. Bernstein, and M. R. Pederson, *Phys. Rev. B* **66**, 092403 (2002).
- [13] D. W. Boukhvalov, A. I. Lichtenstein, V. V. Dobrovitski, M. I. Katsnelson, B. N. Harmon, V. V. Mazurenko, and V. I. Anisimov, *Phys. Rev. B* **65**, 184435 (2002).
- [14] K. Park and M. R. Pederson, *Phys. Rev. B* **70**, 054414 (2004).
- [15] R. Sessoli, H. L. Tsai, A. R. S. S. Wang, J. B. Vincent, K. Folting, D. Gatteschi, G. Christou, and D. Hendrickson, *J. Am. Chem. Soc.* **115**, 1804 (1993).
- [16] K. Takeda and K. Awaga, *Phys. Rev. B* **56**, 14560 (1997).
- [17] S. M. J. Aubin, Z. Sun, L. Pardi, J. Krzystek, K. Folting, L.-C. Brunel, A. L. Rheingold, G. Christou, and D. N. Hendrickson, *Inorg. Chem.* **38**, 5329 (1999).
- [18] M. Soler, S. K. Chandra, D. Ruiz, E. R. Davidson, D. N. Hendrickson, and G. Christou, *Chem. Commun.* **24**, 2417 (2000).
- [19] M. Soler, S. K. Chandra, D. Ruiz, J. C. Huffman, D. N. Hendrickson, and G. Christou, *Polyhedron* **20**, 1279 (2001).
- [20] T. Kuroda-Sowa, M. Lam, A. L. Rheingold, C. Frommen, W. M. Reiff, M. Nakano, J. Yoo, A. L. M. L. C. Brunel, G. Christou, and D. N. Hendrickson, *Inorg. Chem.* **40**, 6469 (2001).
- [21] E. Coronado, A. Forment-Aliaga, A. Gaita-Ariano, C. Guimenez-Saiz, F. Romero, and W. Wernsdorfer, *Angew. Chem. Int. Ed.* **43**, 6152 (2004).
- [22] A. Thielmann, M. H. Hettler, J. König, and G. Schön, *Phys. Rev. B* **68**, 115105 (2003).

- [23] D. Weinmann, W. Häusler, and B. Kramer, Phys. Rev. Lett. **74**, 984 (1995).
- [24] W. Wernsdorfer, R. Sessoli, A. Caneschi, D. Gatteschi, and A. Cornia, Eur. Phys. Lett. **50**, 552 (2000).
- [25] This phenomenon occurs also for higher spin and weak distorted anisotropies ($D^{(0)} \approx D^{(1)}$).
- [26] C. Timm and F. Elste, cond-mat/0511291.
- [27] See also E. Bonet, M. M. Deshmukh and D. C. Ralph, Phys. Rev. **65**, 045317 (2002) for a phenomenologic approach to shifting resonances.
- [28] V. N. Golovach and D. Loss, Phys. Rev. B **69**, 245327 (2004).
- [29] W. Belzig, Phys. Rev. B **71**, 161301(R) (2005).